J Appl Electrochem (2008) 38:1647–1652
DOI 10.1007/s10800-008-9611-6

ORIGINAL PAPER

Effects of substituents of imidazolium cations on the performance of dye-sensitized TiO_2 solar cells

**Kyung Mo Son · Man Gu Kang · R. Vittal ·
Jiwon Lee · Kang-Jin Kim**

Received: 31 October 2007 / Accepted: 20 May 2008 / Published online: 31 May 2008

Abstract Imidazolium iodides (Im^+I^-s) were synthesized with different substituents of the cation and used as electrolytes in dye-sensitized solar cells (DSSCs), and the effects of such substituents were investigated in terms of the photovoltaic performance of the cells. Synthesized iodides were verified by ^{1}H-NMR. Among the iodides, 1,3-diethylimidazolium iodide enabled a solar energy conversion efficiency of 4.8% for its DSSC, while 1-(4-acetophenyl)-3-ethylimidazolium iodide rendered an efficiency of 3.1% for its cell. In all cases the short-circuit photocurrent (J_{sc}) was found to increase with decrease in size of the substituent, which was also verified to be valid in the case of a quasi-solid state DSSC. Results are explained by the electrostatic interactions between solvated Im^+ and negatively charged species based on the correlation between diffusion coefficients of I^- and I_3^- and J_{sc} values. These explanations are supported by steady-state voltammetry and electrochemical impedance spectroscopy (EIS).

Keywords Solvated imidazolium cation · Dye-sensitized solar cells · Solar energy conversion efficiency · Short-circuit photocurrent · Electrostatic interaction

1 Introduction

Imidazolium iodides (Im^+I^-s) have been used as both iodide sources and electrolytes in DSSCs [1–3]. 1-Methyl-3-hexylimidazolium iodide and 1-hexyl-2,3-dimethyllimidazolium iodide are mostly used. As the energy conversion mechanism involves photoinduced interfacial electron transfer, the nature of Im^+ is expected to play a significant role in a DSSC [4, 5].

A few results have been published recently regarding the influence of Im^+I^-s on the photovoltaic properties of DSSCs. Compared with 1,2-dimethylimidazolium and 1-heptyl-3-vinylimidazolium, Li^+ showed a lower open-circuit voltage and a higher short-circuit photocurrent (J_{sc}), which was attributed to a band edge shift of TiO_2 due to the difference in adsorption of the cations to the TiO_2 surfaces [6, 7]. J_{sc}s of DSSCs increased with increasing alkyl chain up to C7 of 1-alkyl-3-methylimidazolium [8]; the J_{sc} increase was explained by multi-layer adsorption of Im^+ to TiO_2 owing to van der Waals forces of the alkyl chains. Studies with cyclic voltammetry and electrochemical impedance spectroscopy, on the other hand, showed that the DSSC containing KI complex with 18-crown-6 gave a higher J_{sc} than that of a DSSC with 1,2-dimethyl-3-propylimidazolium iodide; this enhanced J_{sc} was explained by the increased reductive activity of I^- arising from increased cation size [9].

Though work has been done on the influence of cations on the performance of DSSCs [4, 6, 10–13], there has been no report regarding the effects of substituents of Im^+. Kawano et al. have reported the performances of DSSCs using a variety of imidazolium compounds with different anions [14]; their focus, however, was not on the substituents of an Im^+ ion. In this paper, we report the effects of substituents of Im^+ on the photocurrent–voltage

---

K. M. Son · R. Vittal · K.-J. Kim (✉)
Department of Chemistry, Korea University, Seoul 136-713, Korea
e-mail: kjkim@korea.ac.kr

M. G. Kang
Electronics and Telecommunications Research Institute, Daejeon 305-350, Korea

J. Lee
Samsung SDI Co. Ltd., Gyeonggi-Do 449-577, Korea

characteristics of DSSCs. The results are discussed in terms of electrostatic interactions between solvated Im$^+$ and charge carriers, based on diffusion data obtained by cyclic voltammetry and on charge-transfer resistance measured by EIS. The role of substituents was also vindicated in the case of a quasi-solid state DSSC fabricated with an inorganic–organic hybrid gel electrolyte.

2 Experimental

2.1 Preparation of Im$^+$I$^-$s

Figure 1 shows the Im$^+$I$^-$s used: Iodides of 1,3-diethylimidazolium (Im$^+$ **1**), 1-ethyl-3-methylimidazolium (Im$^+$ **2**), 1-ethyl-3-vinylimidazolium (Im$^+$ **3**), 1-(4-acetophenyl)-3-ethylimidazolium (Im$^+$ **4**), and 1-hexyl-3-methylimidazolium (Im$^+$ **5**) were synthesized. 1-Hexyl-2,3-dimethylidazolium iodide (Im$^+$ **6**) was purchased from Aldrich. Iodides of Im$^+$ **1**, Im$^+$ **5** and Im$^+$ **6** are liquids and the others are solids. Typically Im$^+$ **5** iodide was synthesized as follows: 20 mL of 1-methylimidazole (Aldrich, 99+%) and 200 mL of trichloroethylene (Aldrich, 99+%) were placed in a 3-neck flask in which 40 mL of 1-iodohexane (Aldrich, 97%) was dropped at a rate of one drop per second under N_2 atmosphere. The solution was heated for 3 h at 70 °C under vigorous stirring. Two liquid phases were formed during this process. The required product was collected by the difference in polarity using a separating funnel and washed with trichloroethylene to remove the unreacted reagents [15]. In the case of solid iodides of Im$^+$ **2**, Im$^+$ **3** and Im$^+$ **4**, the products were filtered by suction, washed and vacuum dried for 1 day. All the Im$^+$I$^-$s were confirmed by ^{1}H-NMR (Varian, Mercury NMR 300 MHz), using $CDCl_3$ as a solvent.

2.2 Fabrication and characterization of DSSCs

DSSCs were fabricated according to the procedure described elsewhere [16]. N3 dye was used and the redox electrolyte was composed of 0.04 M I_2 and 0.6 M Im$^+$I$^-$ in 3-methoxypropionitrile (3-MPN). The use of common additives, such as LiI and 4-*tert*-butylpyridine, was avoided. The DSSCs were characterized using a Keithley M 236 source unit. A 300 W Xe lamp with an AM 1.5 filter (Oriel) was used to illuminate the cells at 100 mW cm^{-2}. Electrochemical impedance spectra were recorded with an M1025 frequency-response detector, connected to an EG&G PARC M273A potentiostat. A small ac potential was applied to the electrochemical system consisting of an N3-coated TiO_2 electrode and a Pt counter electrode in 3-MPN, containing 0.6 M Im$^+$I$^-$ and 0.04 M I_2. The complex impedance was measured over 10^5 to 10^{-2} Hz with an ac amplitude of 5 mV. Diffusion coefficients of I^- and I_3^- were obtained by cyclic voltammetry with an EG&G PARC 263A potentiostat using a Pt microelectrode (10-μm diameter), a Pt wire counter electrode, and a Pt wire reference electrode. To measure standard reduction potentials, cyclic voltammograms of the solutions, each containing 0.6 M Im$^+$I$^-$ and 0.1 M tetrabutylammonium perchlorate in 3-MPN, were obtained with an EG&G PARC 263A potentiostat, using a Pt microelectrode (2-mm diameter), a Pt auxiliary electrode, and an Ag/AgCl reference electrode.

2.3 Fabrication of a quasi-solid state DSSC

A quasi-solid state DSSC with Im$^+$I$^-$ was prepared as follows: 3 mL of tetraethyl orthosilicate, 0.4 mL of glacial acetic acid and 0.5 mL of water were mixed together and the content was sonicated for 15 min. 0.3 mL of poly(ethylene glycol) (MW 200, d = 1.127 g cm^{-3}) was then added and the sonication was continued for 10 min more [17]. To the contents 7 mL of the redox electrolyte, containing 0.04 M I_2, 0.6 M Im$^+$I$^-$ in 3-MPN, was added. This gel electrolyte was introduced into the cell through one of the two holes drilled in the counter electrode, followed by sealing of the holes using microcover glass and Surlyn [16].

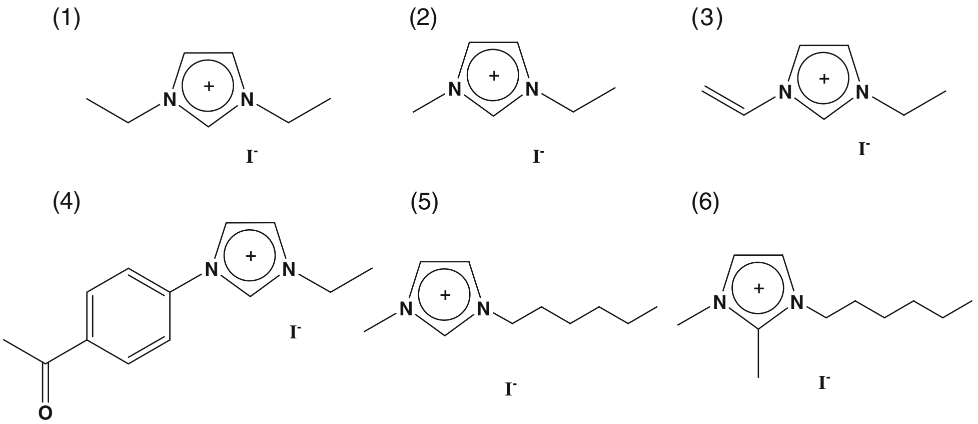

Fig. 1 Iodides of (1) 1,3-diethylimidazolium (Im$^+$ **1**), (2) 1-ethyl-3-methylimidazolium (Im$^+$ **2**), (3) 1-ethyl-3-vinylimidazolium (Im$^+$ **3**), (4) 1-(4-acetophenyl)-3-ethylimidazolium (Im$^+$ **4**), (5) 1-hexyl-3-methylimidazolium (Im$^+$ **5**), and (6) 1-hexyl-2,3-dimethylidazolium (Im$^+$ **6**)

3 Results and discussion

3.1 ^{1}H-NMR spectra of Im^+I^-

Figure 2 shows a well-separated ^{1}H-NMR spectrum of iodide of Im^+ **2**, where all the peaks are indexed from 0 to 10 ppm. The peaks at 4.39–4.46 ppm are assigned to methylene protons and the peak at 4.13 ppm to methyl protons, in which the methylene and methyl groups are linked to the two nitrogens of the ring. The protons within the ring are confirmed from the peaks lying at 7.54 and 10.0 ppm. CH_3 protons of ethyl group appear at 1.61–1.66 ppm. Other synthesized Im^+I^-s were similarly identified.

3.2 Photovoltaic parameters

Figure 3 shows the photocurrent–voltage (*J*–*V*) curves of DSSCs with the six Im^+I^-s as electrolytes. Corresponding short-circuit photocurrent (J_{sc}), open-circuit voltage (V_{oc}), fill factor (FF) and solar-to-electricity conversion efficiency (η) are summarized in Table 1. The results indicate that the J_{sc}s strongly depend on the substituents of the Im^+ cations. Except in the cases of Im^+ **5** and Im^+ **6** that have hexyl chains, the V_{oc}s are nearly the same.

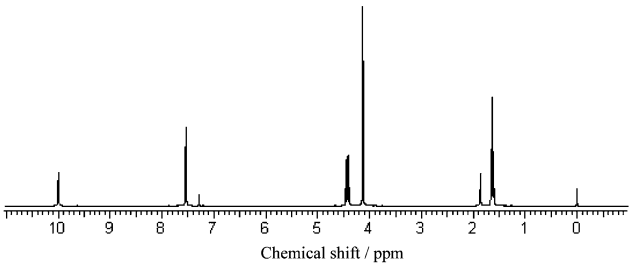

Fig. 2 ^{1}H-NMR spectrum of 1-ethyl-3-methylimidazolium iodide

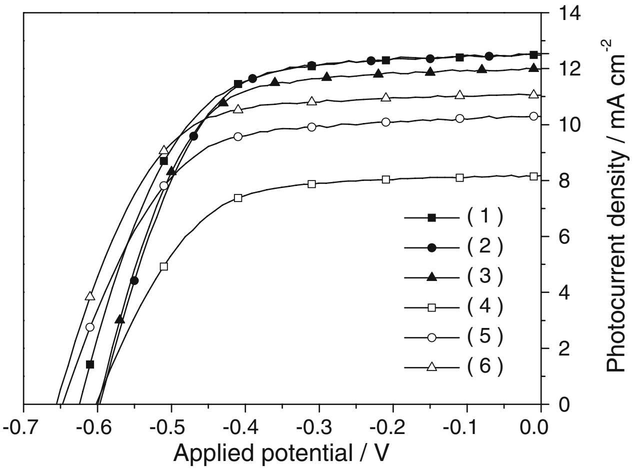

Fig. 3 *J*–*V* curves of DSSCs with electrolytes containing Im^+I^-s with numbers as given in Fig. 1. Light intensity: 100 mW cm^{-2}

Table 1 Photovoltaic parameters of DSSCs[a]

Im^{+b}	J_{sc} (mA cm^{-2})	V_{oc} (V)	FF	η (%)
Im^+ **1**	12.5	0.62	0.63	4.8
Im^+ **2**	12.5	0.60	0.63	4.7
Im^+ **3**	12.0	0.60	0.65	4.7
Im^+ **4**	8.2	0.60	0.62	3.1
Im^+ **5**	10.3	0.65	0.62	4.2
Im^+ **6**	11.1	0.66	0.64	4.7

[a] Each electrolyte consisted of 0.04 M iodine and 0.6 M Im^+I^- in 3-methoxypropionitrile

[b] See Fig. 1

3.3 Behavior of J_{sc}s

As listed in Table 1, the smaller the substituent, the larger the J_{sc}. Im^+ **2** and Im^+ **1** show the highest J_{sc}s, and Im^+ **4** shows the lowest J_{sc}. From the viewpoint of size of the substituent, this tendency is in agreement with reports that a higher J_{sc} was observed in the presence of Li^+ ions compared to that with Im^+ [6, 7].

In order to understand the J_{sc} behavior, we consider the generally accepted charge transfer mechanism for a DSSC, as illustrated in Fig. 4. The mechanism is especially suitable for cells with ionic liquid electrolytes with high ionic strength [1, 18], where electron hopping (ambipolar diffusion) in the TiO_2 film and Grotthuss-type polyiodides bond exchange in the electrolyte are involved [19]. To verify whether diffusion of I^- and I_3^- causes the variations of the photovoltaic properties, we measured their apparent diffusion coefficients (D_{app}s) by cyclic voltammetry. Figure 5 shows comparative steady-state voltammograms in a potential window covering both the reduction of I_3^- and oxidation of I^-, each containing 0.6 M Im^+I^- and 0.04 M I_2 in 3-MPN, which is the same electrolyte composition as that of DSSCs. The D_{app}s of I^- and I_3^- in the electrolytes were calculated from the respective steady-state currents using the following equation,

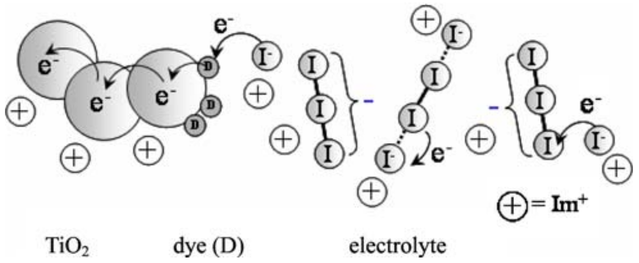

Fig. 4 Schematic representation of charge transfer mechanism for a DSSC with ionic liquid electrolyte

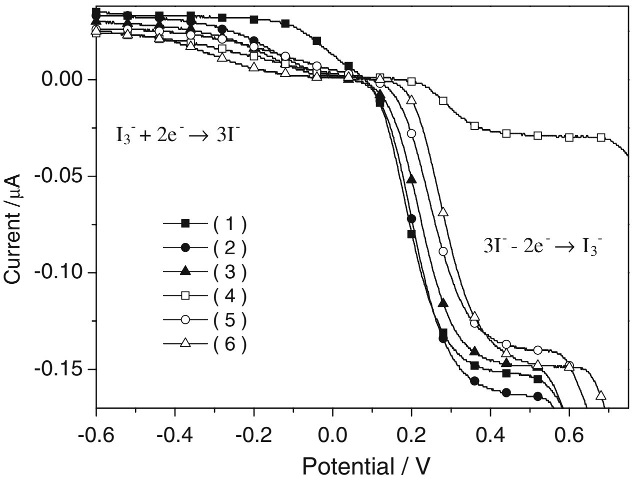

Fig. 5 Steady-state current–voltage curves of a cell with a Pt microelectrode of 10-μm diameter for different Im^+I^-s with numbers as given in Fig. 1. Each electrolyte contained 0.6 M Im^+I^-, 0.04 M I_2 in 3-MPN. Scan rate: 10 mV s^{-1}

$$I_{\mathrm{lim}} = 4nFD_{\mathrm{app}}rC, \quad (1)$$

where I_{lim} is the limiting current, n is the number of electrons transferred per molecule in the oxidation event, F is the Faraday constant, r is the radius of the microelectrode and C is the bulk concentration of electroactive species. The resulting D_{app} of I^- are correlated with corresponding J_{sc} in Fig. 6, which shows that the J_{sc} generally increase with the increase in D_{app}. A similar trend was observed in the case of D_{app} of I_3^- ions with regard to J_{sc}.

Figure 6 also reveals that in general the larger the substituent, the smaller the D_{app} of the I^-. It is assumed that all Im^+ were solvated, because the mole fraction of Im^+ was below 0.06 and the number of the solvent molecules were in excess [20]. When the substituent is large, the corresponding solvated Im^+ is considered to be small and its charge density to be large; movement of I^- ions under such large charge density is assumed to be slower, causing smaller D_{app} of the I^-. Thus solvated Im^+ **1** and Im^+ **2** are expected to be larger than solvated Im^+ **4**, enabling I^- to move faster than Im^+ **4**. This faster movement of iodides leads to increase in D_{app} and enhancement of J_{sc} for Im^+ **1** or Im^+ **2**, relative to that for Im^+ **4**. In addition, the weaker electrostatic interactions between solvated Im^+ **1** or Im^+ **2** and injected electrons in the TiO_2 film lead to faster electron diffusion through the film, which also contributes to the increase in J_{sc}, compared with that in the case of Im^+ **4**. Furthermore, electron transfer from I^- to the oxidized dye molecule appears to be easier at the TiO_2/electrolyte interface, when I^- is less strongly bound to Im^+, contributing to an enhancement of J_{sc}. Similarly, Im^+ **5** or Im^+ **6** is probably more solvated than Im^+ **4**, resulting in the higher J_{sc}s for their cells than that for the cell with Im^+ **4**. Furthermore, because Im^+ **5** and Im^+ **6** have larger hydrophobic chains, larger in sizes but smaller in solvated sizes than Im^+ **1**, Im^+ **2** and Im^+ **3**, the lower J_{sc}s with Im^+ **5** and Im^+ **6** relative to those with Im^+ **1**, Im^+ **2** and Im^+ **3** may be explained. In the presence of a vinyl group, Im^+ **3** is expected to be slightly less solvated than Im^+ **1** or Im^+ **2**; thus its interactions with I^- or I_3^- may be somewhat higher than those of Im^+ **1** or Im^+ **2** with I^- or $I_3{}^-$, which explains the rather lower J_{sc} in its case than those in the cases of Im^+ **1** and Im^+ **2**.

The J_{sc}s behavior was complemented by EIS. Figure 7 compares Nyquist plots of the DSSCs with different Im^+I^-s. The semicircles represent the impedances related to charge transfer processes in the cells. The plots suggest that the charge transfer resistance (R_{ct}) of a cell increases with increase in size of the substituent. The R_{ct} is mainly

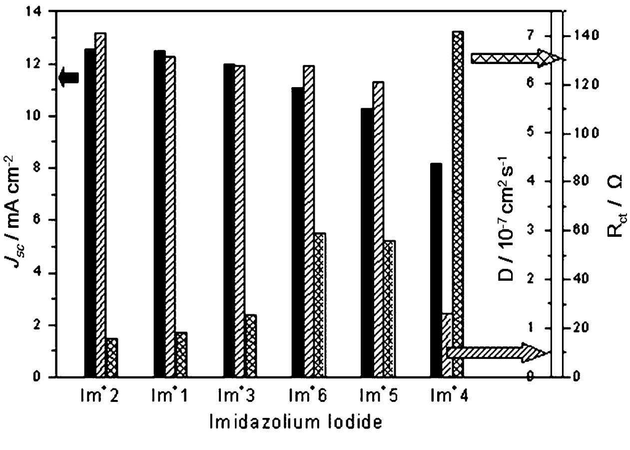

Fig. 6 Dependence of the J_{sc}s of DSSCs with electrolytes containing different Im^+I^-s on the diffusion coefficients (D_{app}s) of respective iodides and on the charge transfer resistances (R_{ct}s) of the respective cells

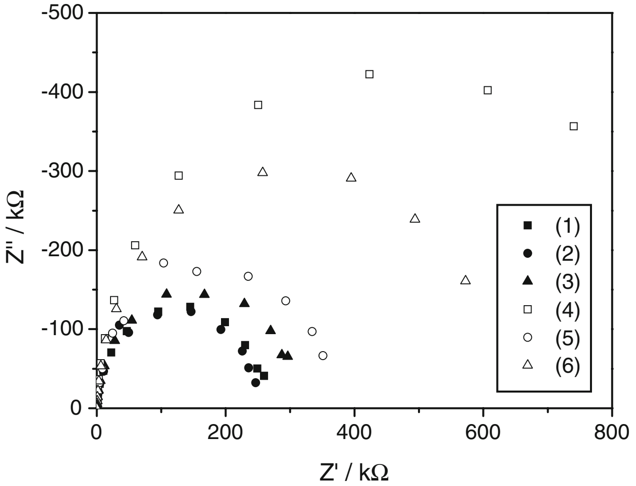

Fig. 7 Nyquist plots of DSSCs, recorded over 10^5 to 10^{-2} Hz, with ac amplitude of 5 mV. Spectra of the six Im^+I^-s are represented by different symbols with numbers as given in Fig. 1

related to the components of resistance for electron transfer from I^- to the oxidized dye molecules and of that for electron transfer from the counter electrode to I_3^-. A small R_{ct} indicates facile electron transfer [21]. Among others, Fig. 6 also demonstrates that the R_{ct} correlate inversely well with the $J_{sc,}$ which is attributable to electrostatic interactions between solvated Im^+ and I^-, as discussed above. In the case of larger substituents, the cations are less solvated, have increased charge density and the electrostatic interactions between them and I^-/I_3^- increase. Therefore in such cases, sluggish electron transfer is expected from I^- to the oxidized dye and from the Pt counter electrode to I_3^-, resulting in a decrease in J_{sc}.

3.4 Alternate interpretation of the published results

The above interpretation may be applied to published results [6–9]. The J_{sc} enhancement with Li^+ compared with that with Im^+ can be interpreted in terms of their solvated sizes [6, 7]. Since Li^+ are more solvated in acetonitrile, the larger solvated Li^+ facilitate an enhanced J_{sc} than Im^+. Similarly, compared to the KI complex with 18-crown-6, the 1,2-dimethyl-3-propylimidazolium has higher electrostatic interaction with I^- in 3-MPN and, therefore, a lower J_{sc} for the DSSC with the latter (instead of a simple size effect) [9]. In the case of a quasi-solid-state electrolyte containing no solvent, the increase in J_{sc} with increase in Im^+ chain length [8] may also be explained. In the absence of organic solvent, the size of the Im^+ is to be considered in its non-solvated form. Under this condition the larger Im^+ imparts weaker electrostatic attraction towards I^- than a smaller Im^+, and thereby facilitates higher J_{sc} for its DSSC than that of a DSSC with a smaller Im^+.

3.5 Behavior of V_{oc}s

Table 1 shows that the V_{oc}s with Im^+ **5** and Im^+ **6** are larger than that of any cell with other Im^+s. It is known that Im^+ is adsorbed on the TiO_2 surface [4] and that adsorption of cations changes its conduction band edge positively [22]. A positive shift causes a decrease in the V_{oc}. Thus, a lower degree of adsorption of solvated Im^+ is desirable for larger V_{oc}. Im^+ **5** and Im^+ **6** with larger charge densities than those of other Im^+s are expected to adsorb to a lesser degree on to the positive sites of the TiO_2 surface, which causes larger V_{oc}s for their DSSCs, relative to those of cells with other Im^+s. Furthermore, the hexyl chains of Im^+ **5** and Im^+ **6** can interact laterally to form an aliphatic network, which can impair the back electron transfer from the conduction band of TiO_2 to the I_3^- [23, 24]. Kubo et al. have observed that electron recombination life time (τ) increases with increase in the alkyl chain length of different Im^+I^-s in DSSCs [5]. This supports the higher V_{oc}s with Im^+ **5** and Im^+ **6**, relative to those of the other Im^+s. These two cations are expected to have longer τ values, which imply reduced recombination reactions and higher V_{oc}s for their DSSCs. However, the variation of V_{oc} in Table 1 appears to have no correlation with the standard reduction potential of the I_3^-/I^- redox couple, because the anodic and cathodic peak potentials, measured by cyclic voltammetry, are essentially the same for all Im^+I^-s in 3-MPN, each containing the respective Im^+ and tetrabutylammonium perchlorate.

3.6 *J–V* curves of a quasi-solid state DSSCs

It can be seen in Table 1 that Im^+ **1** gives a conversion efficiency of 4.8%, while Im^+ **4** gives 3.1%. The conversion efficiency of a DSSC containing Im^+ with a small substituent, such as Im^+ **1** or Im^+ **2** is comparable to that obtainable with a cell with Im^+ **6**. It was interesting to verify whether this observation holds good for a quasi-solid state DSSC. For this purpose we introduced two different Im^+ with a large difference in the size of their substituents, Im^+ **2** and Im^+ **6**, into the inorganic–organic hybrid gel electrolyte, which was prepared as described in the Experimental section. *J–V* curves of pertinent DSSCs shown in Fig. 8 demonstrates that in the viscous hybrid gel electrolyte, a smaller substituent leads to an enhanced J_{sc} of 11.78 mA cm^{-2} relative to that of 10.57 mA cm^{-2} obtained with a larger substituent. This type of J_{sc} behavior is consistent with that shown in Table 1 with respect to the same Im^+s. Table 1 shows the V_{oc} to be 0.60 and 0.66 V for the DSSCs with Im^+ **2** and Im^+ **6**, respectively. For the same Im^+s the V_{oc} is 0.59 V in quasi-solid state DSSCs. This invariance of V_{oc} and its reduced value in the

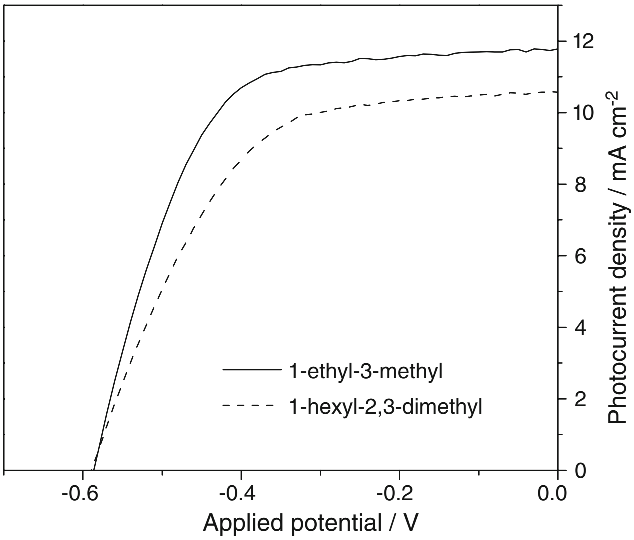

Fig. 8 *J–V* curves of quasi-solid state DSSCs with hybrid gel electrolytes, containing Im^+ **2** (solid curve) and Im^+ **6** (dotted curve) in 3-MPN

quasi-solid state DSSC, relative to those of liquid electrolyte DSSCs with Im^+ **2** and Im^+ **6** (Table 1), may be attributed to lack of formation of an aliphatic network by the substituents around the TiO_2 surface in the hybrid gel electrolyte owing to its gel nature. The fill factors are 0.62 and 0.56 and the conversion efficiencies are 4.3% and 3.5% for the quasi-solid state DSSCs with Im^+ **2** and Im^+ **6**, respectively. These J_{sc} and FF enhancements in quasi-solid state DSSC with Im^+ **2** yielded an improvement in conversion efficiency of DSSC by 24% relative to that of cell with Im^+ **6**. Thus, with respect to the substituents, the J_{sc} behavior of a quasi-solid state DSSC, containing a solvent, is similar to that of a DSSC with a liquid electrolyte.

3.7 Other factors

It is noted in Table 1 that the fill factors are not significantly affected by the substituents. Fill factor is a measure of conductivity of an electrolyte in a DSSC which, in turn, depends on its viscosity. It appears therefore that the viscosity of the electrolytes with mole fraction of Im^+I^- below 0.06 is not affected significantly by the substituents.

Finally, we have not optimized the cells, because the focus of this research was to study changes in the performance of DSSCs caused by varying the substituent of Im^+. For example, we avoided LiI and other additives, e.g., 4-*tert*-butylpyridine, guanidinium thiocyanate, *N*-methylbenzimidazole and nanoparticles. These additives have been reported to be beneficial for optimizing the performance of a DSSC [14, 25–27].

4 Conclusions

Imidazolium iodides (Im^+I^-s) with different substituents were synthesized and identified by ^{1}H-NMR. These Im^+ cations influenced considerably the J_{sc}, and insignificantly the V_{oc} and fill factor. Among them, 1,3-diethylimidazolium showed a conversion efficiency of 4.8%, while 1-(4-acetophenyl)-3-ethylimidazolium gave 3.1% for their respective cells. The smaller the size of the substituent, the faster the apparent diffusion coefficients of I^- and I_3^- and the larger the corresponding J_{sc}. The J_{sc} behavior is interpreted in terms of electrostatic interactions between solvated Im^+ and charge carriers in the electrolyte solution and between solvated Im^+ and electrons in the TiO_2 film. At the TiO_2/electrolyte interface electron transfer from I^- to the oxidized dye molecule appears to be easier when I^- is less strongly bound to Im^+. Complementarily it has been found that the larger the substituent, the larger the corresponding charge transfer resistance and the smaller the J_{sc}. Im^+ with long alkyl chains enabled an increase in V_{oc}, owing to the increased hydrophobic interactions of the alkyl chains to form barriers for back electron transfer reactions. With respect to these substituents, quasi-solid state DSSC, containing an inorganic–organic hybrid gel and a solvent in its electrolyte, shows the same J_{sc} behavior as that of a DSSC containing liquid electrolyte.

Acknowledgments This work was supported by the New and Renewable Energy Research and Development Project under contract 2006-N-PV12-P-05.

References

1. Papageorgiou N, Athanassov Y, Armand M, Bonhote P, Pettersson H, Azam A, Grätzel M (1996) J Electrochem Soc 143:3099
2. Matsumoto H, Matsuda T, Tsuda T, Hagiwara R, Ito Y, Miyazaki Y (2001) Chem Lett 30:26
3. Stathatos E, Lianos P, Zakeeruddin SM, Liska P, Grätzel M (2003) Chem Mater 15:1825
4. Kambe S, Nakade S, Kitamura T, Wada Y, Yanigada S (2002) J Phys Chem B 106:2967
5. Kubo W, Kambe S, Nakade S, Kitamura T, Hanabusa K, Wada Y, Yanagida S (2003) J Phys Chem B 107:4374
6. Park NG, Chang SH, van de Lagemaat J, Kim KJ, Frank AJ (2000) Bull Korean Chem Soc 21:985
7. Kang MG, Ryu KS, Chang SH, Park NG (2004) ETRI J 26:647
8. Kubo W, Kitamura T, Hanabusa K, Wada Y, Yanagida S (2002) Chem Commun 374
9. Shi C, Dai S, Wang K, Pan X, Zeng L, Hu L, Kong F, Guo L (2005) Electrochim Acta 50:2597
10. Liu Y, Hagfeldt A, Xiao XR, Lindquist SE (1998) Sol Energy Mater Sol Cells 55:267
11. Hara K, Horiguchi T, Kinoshita T, Sayama K, Arakawa H (2001) Sol Energy Mater Sol Cells 70:151
12. Watson DF, Meyer GJ (2004) Coord Chem Rev 248:1391
13. Nakade S, Kanzaki T, Kubo W, Kitamura T, Wada Y, Yanagida S (2005) J Phys Chem B 109:3480
14. Kawano R, Matsui H, Matsuyama C, Sato A, Susan MdABH, Tanabe N, Watanabe M (2004) J Photochem Photobiol A Chem 164:87
15. Ohno H (2001) Electrochim Acta 46:1407
16. Kang MG, Park NG, Kim KM, Ryu KS, Chang SH, Hong JS, Kim KJ (2004) J Electrochem Soc 151:E257
17. Stathatos E, Lianos P, Krontiras C (2001) J Phys Chem B 105:3486
18. Kawano R, Watanabe M (2005) Chem Commun 2107
19. Kopidakis N, Schiff EA, Park NG, van de Lagemaat J, Frank AJ (2000) J Phys Chem B 104:3930
20. Chagnes A, Allouchi H, Carré B, Lemordant D (2005) Solid State Ionics 176:1419
21. Bard AJ, Faulkner LR (1980) Electrochemical methods: fundamentals and applications. Wiley, New York
22. Redmond G, Fitzmaurice D (1993) J Phys Chem 97:1426
23. Lagref JJ, Nazeeruddin MdK, Grätzel M (2003) Synth Met 138:333
24. Wang P, Zakeeruddin SM, Moser JE, Grätzel M (2003) J Phys Chem B 107:13280
25. Grätzel M (2004) J Photochem Photobiol A Chem 164:3
26. Wang P, Klein C, Humphry-Baker R, Zakeeruddin SM, Grätzel M (2005) Appl Phys Lett 86:123508
27. Usui H, Matsui H, Tanabe N, Yanagida S (2004) J Photochem Photobiol A Chem 164:97